

Fig. 1. Concentrations of cloud condensation nuclei at 1 percent supersaturation measured during the fire.

(6) at the site of the fire prior to ignition. The counter was then moved to a ridge about 2.5 km downwind of the fire where measurements were taken just before ignition and during the fire (Fig. 1).

The concentration of CCN at the site of the fire an hour before ignition was 50 cm^{-3} at 1 percent supersaturation, and the concentration of CCN at the ridge a few minutes before ignition was about 100 cm^{-3} at 1 percent supersaturation. These relatively low concentrations for land measurements are probably attributable to the proximity of the Pacific Ocean (130 km) and the transport of only slightly modified maritime air to the site of the fire by the prevailing wind (WSW). The variations in CCN count at 1 percent supersaturation measured at the ridge closely followed the intensity of the fire (Fig. 1).

Measurements of the concentrations of CCN at several different supersaturations taken at the ridge before the fire was lit and during the fire (Fig. 2) show that the fire was a significant source of only relatively inefficient CCN. Extrapolation of the supersaturation spectrum taken during the fire shows that the number of CCN active at 0.2 per-

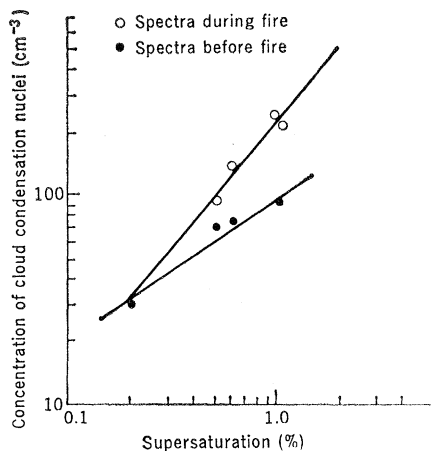


Fig. 2. Supersaturation spectra of cloud condensation nuclei before and during the fire.

cent supersaturation was unchanged by the fire at this stage.

These observations indicate that the burning of forest products can generate large concentrations of CCN active at about 1 percent supersaturation. However, in order to estimate better the importance of forest fires as sources of CCN, measurements should be made in the vicinity of various types of large forest fires.

PETER V. HOBBS
L. F. RADKE

*Cloud Physics Laboratory,
Department of Atmospheric Sciences,
University of Washington, Seattle 98105*

References and Notes

1. P. Squires and S. Twomey, *Tellus* **10**, 272 (1958).
2. S. Twomey, *Bull. Observ. Puy de Dome* **1**, 1 (1960).
3. P. Squires, *J. Rech. Atmos.* **2**, 297 (1966).
4. J. Warner and S. Twomey, *J. Atmos. Sci.* **24**, 704 (1967).
5. J. Warner, *J. Appl. Meteorol.* **7**, 247 (1968).
6. L. F. Radke and P. V. Hobbs, in *Proc. Int. Conf. Cloud Physics* (Toronto, 1968), p. 35.
7. The simulated forest fire at Pack Forest was supported by a grant to the College of Forestry, University of Washington, from the U.S. Forest Service grant 4040. The measurements were supported by contract 14-06-D-5970 from the Office of Atmospheric Water Resources, U.S. Department of Interior. Contribution 172 from the Department of Atmospheric Sciences, Univ. of Washington, Seattle.

19 August 1968

Role of Surface Dipoles on Axon Membrane

Abstract. *A physical model of nerve excitation and conduction is proposed based on the discovery of three new axon membrane properties: the negative fixed surface charge, the birefringence change, and the infrared emission.*

The mechanisms of nerve excitation and conduction have not been well understood mainly because little is known about the intrinsic physical properties of axon membrane. Recently

(April–June 1968), there were three developments. Segal has shown the existence of negative, fixed surface charges on the giant axons of squid and lobster (1). The minimum values of the

charge densities determined were 1.9×10^{-8} and 4.2×10^{-8} coul/cm², respectively. He also found no evidence that the properties of the shear surface were altered by the loss of resting potential. Cohen, Keynes, and Hille have shown conclusively that there was a birefringence change that coincided with the action potential in a squid giant axon (2). It follows from their experiments that the birefringence change has a radial optical axis and that it arises from sources arranged in a cylindrical region at the outer edge of the axon or in the sheath. Fraser and Frey have detected infrared emission—intensity of $6 \mu\text{W}/\text{cm}^2$ —from active live crab nerves. This emission exceeded the blackbody radiation and the stimulus artifact heating by two orders of magnitude and therefore must be located at the surface of the nerve (3). The significance of these three new findings is so profound that we wish to explore it at some length in this communication.

An immediate question following Segal's finding is whether there would be fixed charge on the inner surface of the axon. Since the resting potential is positive outside, and since the ionic solutions are conducting media in which the potential change, if any, would be rather small, Segal's result would imply that neutral or positive charge on the inner surface of the axon would be very unlikely, because otherwise the resting potential would be opposite to that observed. The only possibility then is that there might be negative fixed charge on the inner surface of the axon. In order to keep the negative charges on both surfaces (70 Å apart) from repelling each other and also to fulfill the neutrality condition, there must be a positively charged layer standing close to the negative surface charge on each side. Therefore, there would be two dipole layers on the inner and the outer sides of the axon membrane, with their negative ends facing the aqueous phases.

With these surface dipoles, the potential profile will resemble that shown in Fig. 1. The higher potential in the membrane region will trap anions coming from both sides and thus makes that region N-type in the semiconductor language. This explains the well-known fact that an axon membrane is permselective to anions, because they will have the lowest potential energy ($-qV$) and hence are inclined to stay in the membrane region. On the other hand, cations will have the highest potential energy and hence are rather unstable

in the membrane region. This shows why the membrane is highly permeable to some cations unless they are barred by the high barrier at the interface. The negative surface charge will attract cations in the ionic solution and hence a P-type layer will be formed in the aqueous phase in the immediate vicinity of the negative surface charge on either side. Thus the electrical structure of an axon membrane and its immediate vicinity would look like $P \leftarrow N \rightarrow P$, where the arrows indicate dipole layers and their directions. Such a structure has been suggested previously for a plasma membrane by Danielli and Davson (4), but there was lack of evidence to support it. Now we arrive at the same result for an axon membrane from Segal's finding of the negative surface charge, the polarity of membrane potential, and the coulomb interactions in various regions.

The outer barrier potential E_0 can be calculated as follows.

$$E_0 = \sigma s / \epsilon \quad (1)$$

where σ is the surface charge density, s the barrier width (or dipole length) and ϵ , the permittivity. The barrier width is approximately 10 Å. Taking ϵ as 8.85×10^{-12} farad/m and σ as 1.9×10^{-8} coul/cm² (for squid) from Segal's experiment, we obtain

$$E_0 = -21.4 \text{ mv}$$

This value is in good agreement with the value (-20 mv) estimated by Wei from some other physical arguments (5) and also with those calculated by Johnson, Eyring, and Polissar using various hypothetical values of distribution constants for sodium, potassium, and chloride (6). Our result and that of Johnson *et al.* confirm the idea that the barrier potentials are of the same order of magnitude as the observed membrane potential, and hence the potential profile shown in Fig. 1 is justified. (The observed membrane potential E_R is the algebraic sum of the three potentials E_0 , E_i , and E_M as shown in Fig. 1, where E_0 and E_i are the outer and inner barrier potentials and E_M , the true membrane potential.)

The outer dipole barrier is essential to the understanding of many nerve processes (electrical, optical, and thermal). In the resting state, it is the height of this barrier which bars sodium ions from entering the membrane. Previous calculation by Wei has shown this very clearly (5). If the sodium ions are to move inward, the dipole barrier must be lowered by some

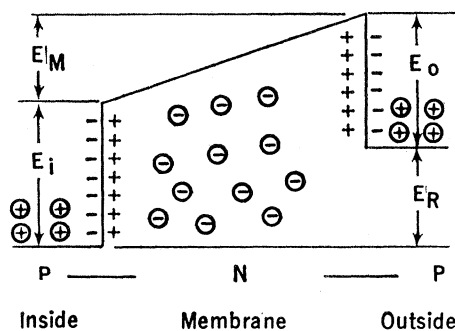


Fig. 1. The potential profile and the $P \leftarrow N \rightarrow P$ structure of axon.

means. The latter condition will lead to "nerve excitation." The fundamental criterion for nerve excitation is that the total driving force (f) on a positive ion at the edge of the outer barrier must be in the inward direction (5), that is,

$$f = f_1 + f_2 + f_3 > 0 \quad (2)$$

where f_1 is the electrical force exerted by the outer barrier; f_2 , the diffusional force; and f_3 , another driving force which may be dominant under special circumstance. A possible way to lower the dipole barrier and hence to fulfill the above criterion is to apply a negative potential gradient to the proximity of the negative poles (surface charges) of the outer dipole layer. If the applied negative potential is sufficient, then some of the dipoles will turn around to the opposite orientation and the barrier potential will be given approximately by

$$E_0 = s Q(N_1 - N_2) / \epsilon \quad (3)$$

where N_1 and N_2 are the population densities of dipoles in the two states (orientations), s , the barrier width, and Q , the charge of a single pole. Thus to lower E_0 , one has to decrease N_1 and increase N_2 , or to excite dipoles from the ground state to the upper state. This can be achieved effectively if the energy conservation law is satisfied,

$$U = pF = E_2 - E_1 \quad (4)$$

where p is the dipole moment; F , the applied field; U , the perturbation energy; and E_1 and E_2 , the energies of the two states. We shall now estimate the field required to satisfy Eq. 4. Under an electric field, a dipole molecule tends to vibrate and rotate. The vibrational states of large molecules generally have energy spacing in the infrared range, or in the order of a few kT . Though we do not know the exact structure of the dipoles at the membrane surface, the general belief is that the membrane interface is composed of

lipoproteins (4, 7). Hence, we take p to be equal to the dipole moment of a protein, which ranges from 170 to 1400 Debye units (8, 9). Thus by letting $E_2 - E_1 = 3 kT$ and $p = 170$ to 1400 debyes, we obtain from Eq. 4

$$F = (2.6 \text{ to } 20) \times 10^4 \text{ volt/cm}$$

For a membrane region of 100 Å, the potential difference required would be 26 to 200 mv, which is entirely practical. In fact, the simplest way to stimulate a nerve axon is to apply a cathodic potential close to the axon outer surface and an anodic potential to the inner surface, with a magnitude less than 200 mv across the membrane. (It is the lowering of the outer barrier by the "depolarizing field" that causes inward flow of sodium or other cations.) Thus, there is a good agreement between theory and experiment.

Equation 4 also implies another important characteristic of nerve excitation, that is, the "all-or-none" response. If the stimulated perturbation energy U is less than $E_2 - E_1$, few dipoles would flip up, then the barrier potential E_0 from Eq. 3 would not be lowered very much and the criterion 2, not fulfilled. Hence no response. If U equals or exceeds $E_2 - E_1$, the response will be "all," in the sense that the response amplitude is relatively independent of U once it exceeds the threshold $E_2 - E_1$. This is quite understandable from the standpoint of quantum transition probability. Thus, the "all-or-none" response may be regarded as a macroscopic expression of quantum transitions of dipoles at the membrane surface.

When the stimulation is removed, the excited dipoles will relax to the ground state. The energy quanta $h\nu = E_2 - E_1 \approx$ a few kT released could appear as heat or infrared emission, or both. Indeed, both have been observed (3, 10). They could also be reabsorbed by the neighboring dipoles which have the same energy levels. Abbott *et al.* did find that 80 percent of the heat produced after the passage of a single nerve impulse was reabsorbed (10). The remaining 20 percent could be radiated as infrared emission. This figure is amazingly close to that (15 percent) estimated by Fraser and Frey from their emission experiment (3).

That the birefringence change coincided with the action potential in a squid axon as found by Cohen *et al.* (2) implies that the optical and the electrical effects must come from the same cause. In our view, the most likely common cause is the dipole reorienta-

tion under an applied electric field. Cohen *et al.* have already suggested that a large part of the birefringence change arose in radially oriented molecules associated with the membrane, and they are not different in nature from the dipoles we have so far discussed. From Langevin's theory, an electric field will induce orientational polarizability of polar molecules and thus change the refractive index of the dielectric (11). Thus the finding by Cohen *et al.* lends a further support to the dipole theory for nerve excitation.

The dipole flip-flop can offer an immediate explanation for the impulse propagation along an axon. Since all dipoles have the same energy levels, dipole flop from energy level E_2 to E_1 at point A will cause dipole flip from energy level E_1 to E_2 at the neighboring point B by the law of conservation of energy. The barrier potential at B would be lowered and a nerve impulse would appear there. This process will go on and on and one sees pulse propagation along the axon.

The comparison of Fig. 1 with the structure and the potential profile of a *p-n-p* transistor shows similarity. In a transistor, the emitter barrier is lowered by applying a forward bias which draws carriers away from the junction. In an axon, the outer barrier is lowered by applying a cathodic potential which causes dipole flipping. Since the physical principles governing the dynamics of charged particles are the same, there is no reason why the axon would not take a transistor action once its outer barrier is lowered. Such a theory was proposed previously by Wei and it did predict many features of nerve conduction (12). However, at that time (1966), there was no evidence for the existence of surface dipoles and hence the exact roles played by surface dipoles were not too clear. Now, in the face of the recent discoveries of axon membrane (physical) properties, the dipole theory appears more plausible and thus may serve as a physical basis for nerve excitation and conduction.

LING Y. WEI

*Biophysical Research Laboratory,
Electrical Engineering Department,
University of Waterloo,
Waterloo, Ontario, Canada*

References and Notes

1. J. R. Segal, *Biophys. J.* **8**, 470 (1968).
2. L. B. Cohen, R. D. Keynes, B. Hille, *Nature* **218**, 438 (1968).
3. A. Fraser and A. H. Frey, *Biophys. J.* **8**, 731 (1968).
4. F. Brown and J. F. Danielli, in *Cytology*

and *Cell Physiology*, G. B. Bourne, Ed. (Academic Press, New York, 1964), p. 249.

5. L. Y. Wei, *Biophys. J.* **8**, 396 (1968).
6. F. H. Johnson, H. Eyring, M. J. Polissar, *The Kinetic Basis of Molecular Biology* (Wiley, New York, 1954), chaps. 11 and 12.
7. J. L. Kavanau, *Structure and Function in Biological Membranes* (Holden-Day, San Francisco, 1965), vol. 1.
8. E. J. Cohen and J. T. Edsall, *Proteins, Amino Acids and Peptides* (Reinhold, New York, 1943).
9. The use of the values of protein dipole moment is merely for the estimating purpose and does not imply that the electric dipoles are

located in the protein covering the membrane surface. At present, to my knowledge, there is no direct evidence to indicate the exact location of electric dipoles. However, this knowledge is not very essential to the present theory which is only concerned with physical principles.

10. B. C. Abbott, J. V. Howarth, J. M. Ritchie, *J. Physiol. (London)* **178**, 368 (1965).
11. C. Kittel, *Introduction to Solid State Physics* (Wiley, New York, 1967), chap. 12.
12. L. Y. Wei, *IEEE Spectrum* **3**, 123 (1966).
13. Supported by the National Research Council of Canada under grant No. A-1252.

5 July 1968; revised 16 October 1968

Structural Stability and Solvent Denaturation of Myoglobin

Abstract. *As judged from the midpoints of the denaturation transition of 31 water-miscible alcohols, ureas, and amides, the effectiveness of these denaturing agents on sperm-whale myoglobin increases with increasing chain length and hydrocarbon content, as expected in view of the disorganization of the hydrophobic interior of this protein. Increase in the hydroxyl content, blocking of the functional amino groups of the ureas and amides by alkyl substitution, and branching of the hydrocarbon portion of the denaturants are of less importance in determining the effectiveness of the denaturants.*

Considerable evidence based on both experimental and theoretical studies has indicated the importance of hydrophobic interactions for altering the native structure of proteins and nucleic acids in solution (1-3). Previously we have examined the effects of various structurally related denaturants on the conformational stability of DNA (4-6). Fairly detailed three-dimensional structures of sperm-whale myoglobin (7) and other proteins (8), which indicate the location of the various amino acid side chains, have been obtained by x-ray crystallography. The systematic investigation of the effectiveness of structurally related denaturing agents, such as the alcohols, ureas, and amides, on these proteins should help to elucidate the nature of those forces controlling native structure. Such studies should also lead to better understanding of hydrophobic bonding or hydrophobic interactions (1-3, 9). We here report on the denaturation of sperm-whale myoglobin by solvents. A brief communication on this subject has been presented, including similar denaturation studies on cytochrome c and α -chymotrypsinogen (10).

The denaturation of proteins and nucleic acids can be readily followed by several techniques. Changes in the optical rotatory dispersion (ORD) of proteins at 233 nm reflect mainly alterations in secondary structure or the breakdown and reformation of the helical organization of proteins upon solvent denaturation (11). On the other hand, changes in the direct spectra, as

well as in the difference spectra of the heme proteins at 409 nm (12) and at 286 to 288 nm (13), reflect alterations in the environment of the heme moiety and the hydrophobic tyrosyl and tryptophyl residues, respectively. The changes in mean residue rotation ($[M]_{233}$), molar absorbance (ϵ_M) at 409 nm, and denaturation difference spectra (expressed as the difference in molar absorbance $\Delta\epsilon_{288}$; measured at 288 nm with $\Delta\epsilon$ at 325 nm taken as zero reference) produced by the addition of such denaturants as urea and propanol (Fig. 1), for example, are closely parallel (14-17) with essentially similar denaturation midpoints, despite the different physical origins of the measured parameters.

The gradual refolding of proteins in helix-promoting solvents above the transition region were first observed by Tanford and co-workers (18) in β -lactoglobulin and γ -globulin. With myoglobin, similar changes are noted in solvents such as propanol (Fig. 1) and other alcohols where the gradual refolding of the polypeptide chain into an altered conformation (1, 2, 18) is accompanied by a gradual change in $[M]_{233}$. Changes in helix content are not accompanied by parallel changes in the environments of the heme and aromatic tryptophyl and tyrosyl chromophores, since no corresponding changes are noted in the ϵ_{409} and $\Delta\epsilon_{288}$ curves. Data obtained with a random coil-promoting solvent, urea (Fig. 1), indicate no comparable conformational effects.